

Elastic scattering loss of atoms from colliding Bose-Einstein condensate wavepackets

Y. B. Band^{1,2} Marek Trippenbach^{2,3}, J. P. Burke Jr.², and P. S. Julienne²

¹ Department of Chemistry, Ben-Gurion University of the Negev, Beer-Sheva, Israel 84105

² Atomic Physics Division, A267 Physics, National Institute of Standards and Technology, Gaithersburg, MD 20899

³ Institute of Experimental Physics, Optics Division, Warsaw University, ul. Hoza 69, Warsaw 00-681, Poland

Bragg diffraction of atoms by light waves has been used to create high momentum components in a Bose-Einstein condensate. Collisions between atoms from two distinct momentum wavepackets cause elastic scattering that can remove a significant fraction of atoms from the wavepackets and cause the formation of a spherical shell of scattered atoms. We develop a slowly varying envelope technique that includes the effects of this loss on the condensate dynamics described by the Gross-Pitaevski equation. Three-dimensional numerical calculations are presented for two experimental situations: passage of a moving daughter condensate through a non-moving parent condensate, and four-wave mixing of matter waves.

A light-induced potential applied to a Bose-Einstein condensate (BEC) can be used to make high momentum daughter BEC wavepackets which propagate through the parent condensate [1–3]. High momentum means very large in relation to the mean momentum in the parent wavepacket and the momentum mv_s where v_s is the sound velocity in the parent. Such techniques have been used to make an atom laser [4], to study the coherence properties of condensates [3,5,6], and to study nonlinear four-wave mixing (4WM) of coherent matter waves [7,8]. As explained in this Letter, elastic scattering between condensate atoms from different momentum wavepackets can remove copious numbers of atoms from these moving wavepackets. Recently, profuse elastic scattering of atoms between daughter and parent BEC wavepackets has been observed at MIT [9]. Such losses will be an important consideration for atom optics applications. Fig. 1 schematically shows wavepackets in momentum space where the high momentum wavepacket with central momentum $\mathbf{P}_2 = 2\hbar\mathbf{k}_{ph}$ was produced by optically-induced Bragg scattering from the $\mathbf{P}_1 = 0$ initial wavepacket. Here $\hbar\mathbf{k}_{ph} = h/\lambda_{ph}$ is the photon momentum for light with wavelength λ_{ph} . The spherical shell in Fig. 1 (excluding the condensate wavepackets) results from elastic scattering between atoms from the \mathbf{P}_1 wavepacket and atoms from the \mathbf{P}_2 wavepacket. The elastically scattered atoms in the spherical shell can neither be described as part of the mean-field of the BEC, nor can the formation [10] or evolution of the spherical shell be modeled using the usual Gross-Pitaevskii equation (GPE) [11], Eq. (1). In what follows we use the term “elastic scattering” to mean *only* those non-forward elastic scattering processes not accounted for within the GPE.

Here we provide a simple means of describing the loss of atoms from the condensate wavepackets due to the elastic scattering mechanism. This is made possible by (a) using the appropriate momentum dependence of the nonlinear coupling constant in the GPE [12,13] and (b) using a newly developed slowly-varying-envelope approximation (SVEA) for the condensate wavefunction in systems with

both slow and fast momentum components [14]. Since the SVEA treats each distinct momentum wavepacket separately, we can incorporate the correct momentum dependence in the nonlinear coupling constants. Thus, we can treat the effect of elastic scattering losses on the condensate dynamics using the SVEA version of the GPE, even in single spin component systems. We first outline the theory for describing elastic scattering loss and then present two examples, one applied to output coupling of atom laser pulses from a BEC source, and the other to 4WM. A more complete discussion of the theory and further applications will be presented elsewhere [15].

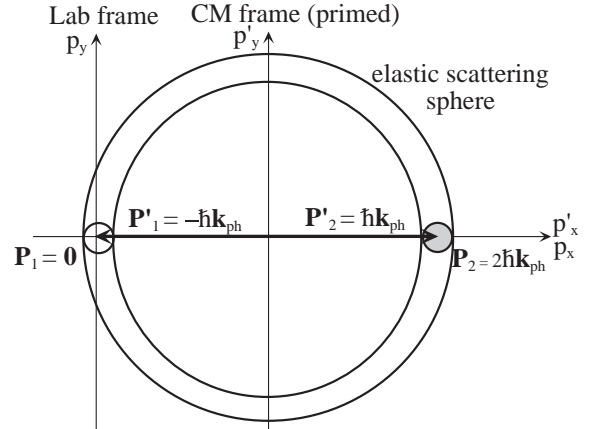


FIG. 1. (a) Wavepackets in momentum space with laboratory frame central momenta $\mathbf{P}_1 = 0$ and $\mathbf{P}_2 = 2\hbar\mathbf{k}_{ph}$ undergoing elastic scattering to produce a spherical shell of elastically scattered particles. In the CM frame moving with velocity $\mathbf{v}_{cm} = \hbar\mathbf{k}_{ph}/m$, momenta are shifted by $-\hbar\mathbf{k}_{ph}$.

The GPE for a single spin component BEC at zero temperature can be written as [11]

$$i\hbar \frac{\partial \Psi}{\partial t} = (T_{\mathbf{x}} + V(\mathbf{x}, t) + U_0 N_T |\Psi|^2) \Psi, \quad (1)$$

where $T_{\mathbf{x}} = \frac{-\hbar^2}{2m} \nabla^2$ is the kinetic energy operator, $V(\mathbf{x}, t)$ is the external trapping potential imposed on the atoms,

N_T is the total number of atoms in the condensate, and Ψ is normalized to unity. Although the coupling constant is usually expressed as $U_0 = \frac{4\pi\hbar^2 a_0}{m}$, where a_0 is the s -wave scattering length and m is the atomic mass, it is more correct at zero temperature to express U_0 in terms of the many-body T -matrix, which is often well-approximated by the 2-body T -matrix [12,13]: $U_0(k) = -\frac{4\pi\hbar^2 T(k)}{mk}$. Here $T = \frac{S-1}{2i}$, S is the unitary S -matrix, and $\hbar k$ is the relative momentum of the colliding atoms. If we assume no inelastic scattering and expand $T(k)/k$ in powers of k using $S(k) = e^{-2ik a_0} + O(k^3)$, we obtain:

$$\frac{T(k)}{k} = -a_0 + ika_0^2 + O(k^2). \quad (2)$$

In a normal condensate, the lead term in Eq. (2) gives the usual GPE. However, if two wavepackets with very different momenta interact (cross-energy terms in Eqs. (6-7)), ka_0 need not be negligible ($ka_0 = 0.06$ for the Na condensate example given below), and the second term in Eq. (2) must be taken into account. This term generates the elastic scattering loss term in the GPE. If we apply the optical theorem to the forward scattering amplitude, it is this second term that is responsible for scattering out of the forward direction. Suitable generalizations of Eq. (2) allow inclusion of inelastic collision losses and treatment of multiple spin-component condensates.

The application of an optical standing wave pulse diffracts a fraction of the initial condensate into a high momentum component [1-3]. To a very good approximation, the wavefunction immediately after application of a set of optical pulses is given by the superposition of wavepackets,

$$\Psi(\mathbf{x}, t = 0) = \psi(\mathbf{x}) \sum_{j=1}^J a_j \exp(i\mathbf{k}_j \cdot \mathbf{x}), \quad (3)$$

where J is the number of distinct momentum wavepackets present. Here $\psi(\mathbf{x})$ is the initial wavefunction of the parent condensate before application of the optical pulses; it is the solution to the GPE with a harmonic potential centered around $\mathbf{x} = \mathbf{0}$. We assume the momentum differences $\hbar|\mathbf{k}_i - \mathbf{k}_j|$ to be much larger than both the momentum spread in the initial parent BEC wavepacket and the momentum mv_s associated with the speed of sound v_s in the BEC (hence, superfluid suppression of collisions [9] does not occur). Since different wavepackets do not overlap in momentum space, $\sum_{j=1}^J |a_j|^2 = 1$.

The SVEA is made by writing the wavefunction as

$$\Psi(\mathbf{x}, t) = \sum_j \Phi_j(\mathbf{x}, t) \exp(i\mathbf{k}_j \mathbf{x} - i\omega_j t). \quad (4)$$

Eq. (4) explicitly separates out the fast oscillating phase factors representing central momentum $\hbar\mathbf{k}_j$ and kinetic energy $E_j = \hbar\omega_j = \hbar k_j^2/2m$ and defines the slowly varying envelopes Φ_j , which vary in time and space on

much slower scales than the phases. Consequently, full three-dimensional (3D) calculations of the envelopes is numerically tractable, as we describe in more detail elsewhere [6,14]. In the first example we consider below, we take only two components, i.e., $j = 1, 2$ and the initial condition is $\Phi_j(\mathbf{x}, t = 0) = a_j \psi(\mathbf{x})$. In the 4WM process, $j = 1, \dots, 4$, with $\Phi_j(\mathbf{x}, t = 0) = a_j \psi(\mathbf{x})$ for $j = 1, 2, 3$, and the $j = 4$ envelope is initially unpopulated, $\Phi_4(\mathbf{x}, t = 0) = 0$. This envelope becomes populated as a result of the coherent 4WM process. Substituting the SVEA form for the wavefunction into the GPE, collecting terms with the same phase factors, multiplying by the complex conjugate of the appropriate phase factors, and neglecting terms that are not phase matched (those for which momentum and energy are not conserved) we obtain a set of coupled SVEA equations for $\Phi_j(\mathbf{x}, t)$:

$$\left(\frac{\partial}{\partial t} + (\hbar\mathbf{k}_j/m) \cdot \nabla + \frac{i}{\hbar} \left(-\frac{\hbar^2}{2m} \nabla^2 + V(\mathbf{r}, t) \right) \right) \Phi_j = -\frac{i}{\hbar} U_0 N_T \sum_{qrs} \delta(\mathbf{k}_{jQRS}) \delta(\omega_{jQRS}) \Phi_q \Phi_r^* \Phi_s. \quad (5)$$

Only phase-matched terms, for which $\mathbf{k}_{jQRS} = \mathbf{k}_j - \mathbf{k}_q + \mathbf{k}_r - \mathbf{k}_s = 0$ and $\omega_{jQRS} = \omega_j - \omega_q + \omega_r - \omega_s = 0$, are retained on the right hand side of Eqs. (5).

For simplicity, we consider explicitly the SVEA equations for the case where only two central momentum components, $\mathbf{0}$ and $2\hbar\mathbf{k}_{ph}$, are present. Then, only ‘‘phase-modulation’’ nonlinear self- and cross-energy interaction terms are present, as opposed to the case when three central momentum components are present and 4WM terms also arise. It is convenient to go to a center of mass frame moving with velocity $\mathbf{v}_{cm} = \hbar\mathbf{k}_{ph}/m$ (see Fig. 1). In this frame, wavepacket 1 has momentum $-\hbar\mathbf{k}_{ph}$, wavepacket 2 has momentum $\hbar\mathbf{k}_{ph}$, and elastic scattering from the $\pm\hbar\mathbf{k}_{ph}$ wavepackets creates a spherical shell expanding in 4π steradians with momentum $|\hbar\mathbf{k}_{elas}| = |\hbar\mathbf{k}_{ph}|$. The SVEA equations in this frame are given explicitly by:

$$\left(\frac{\partial}{\partial t} + (-\mathbf{v}_{cm}) \cdot \nabla + \frac{i}{\hbar} \left(-\frac{\hbar^2}{2m} \nabla^2 + V(\mathbf{r}, t) \right) \right) \Phi_1 = -i \frac{4\pi\hbar a_0}{m} N_T (|\Phi_1|^2 + 2|\Phi_2|^2) \Phi_1 - \frac{(v_{rel})\sigma N_T}{2} |\Phi_2|^2 \Phi_1, \quad (6)$$

$$\left(\frac{\partial}{\partial t} + \mathbf{v}_{cm} \cdot \nabla + \frac{i}{\hbar} \left(-\frac{\hbar^2}{2m} \nabla^2 + V(\mathbf{r}, t) \right) \right) \Phi_2 = -i \frac{4\pi\hbar a_0}{m} N_T (|\Phi_2|^2 + 2|\Phi_1|^2) \Phi_2 - \frac{(v_{rel})\sigma N_T}{2} |\Phi_1|^2 \Phi_2. \quad (7)$$

where $\sigma = 8\pi a_0^2$ and $v_{rel} = 2\hbar k_{ph}/m = 2v_{cm}$ is the relative velocity of the two wavepackets. The factor of 2 multiplying the nonlinear cross-energy interaction terms results from expanding $|\Psi|^2\Psi$ with $\Psi(\mathbf{x}, t) = \sum_{j=1}^2 \Phi_j(\mathbf{x}, t) \exp(i\mathbf{k}_j \mathbf{x} - i\omega_j t)$ and collecting the phase-matched terms appropriately. In the self-energy term proportional to $|\Phi_i|^2\Phi_i$, $i = 1, 2$, only the lead term

in Eq. (2) is retained. However, both terms in Eq. (2) are retained in the cross-energy terms $|\Phi_i|^2\Phi_j$, $i = 1, 2$, $j = 2, 1$, leading to the elastic scattering loss terms proportional to $v_{rel}\sigma$.

The form of the elastic collisional loss terms can also be motivated by a classical hydrodynamic picture of elastic collisions of a cloud of atoms having a central velocity $\mathbf{v}_1 = \mathbf{P}_1/m$ and density $n_1(\mathbf{x}, t)$, with a cloud of atoms having velocity \mathbf{v}_2 and density $n_2(\mathbf{x}, t)$. The atomic densities can be determined from:

$$\frac{\partial n_1(\mathbf{x}, t)}{\partial t} + \mathbf{v}_1 \cdot \nabla n_1(\mathbf{x}, t) = -|\mathbf{v}_1 - \mathbf{v}_2| \sigma n_1 n_2, \quad (8)$$

and a similar equation for $\frac{\partial n_2(\mathbf{x}, t)}{\partial t}$. Thus, elastic scattering takes atoms out of both clouds. For sufficiently slow relative atomic velocities so that only s -wave scattering occurs, and both atoms have the same spin quantum numbers, $\sigma = 8\pi a_0^2$. Here the relative velocity is $v_{rel} = |\mathbf{v}_1 - \mathbf{v}_2| = 2v_{cm}$. The extra factor of $\frac{1}{2}$ in the loss terms in Eqs. (6)-(7) are due to the fact that these are equations for amplitudes (Φ), not densities ($|\Phi|^2$). Inelastic scattering with cross section σ_{in} , if present, is easy to include by replacing σ by $\sigma + \sigma_{in}$.

If we apply this theory to condensates with two spin components, the cross section which appears in the loss term due to collisions between wavepackets of the two different components is $\sigma = 4\pi a_0^2$, as expected from two-body scattering theory for different spin components. In the SVEA derivation this follows from the fact that the cross phase modulation terms are then of the form $-\frac{i}{\hbar}U_0N_T(|\Phi_2^b|^2)\Phi_1^a$, rather than $-\frac{i}{\hbar}U_0N_T(2|\Phi_2^a|^2)\Phi_1^a$ as here (note the factor of 2), where the superscripts a and b denote spin indices.

As a first example, we consider a condensate of Na atoms in the $F = 1$, $M = -1$ Zeeman sublevel in a cigar-shaped trap elongated in the z -direction. After the trapping potential is turned off, the condensate is allowed to freely evolve for 600 μs , and a short duration Bragg scattering pulse is applied that creates a $2\hbar\mathbf{k}_{ph} = (2h/\lambda_{ph})\hat{z}$ momentum component. We consider the case with half the initial atoms in the high momentum component and half in the parent condensate. We evolve the condensate wavepackets using a full 3D implementation of Eqs. (6)-(7) until the wavepackets move apart and are physically separated. Fig. (2) shows N_f/N_T versus the aspect ratio, R_{aspect} , of the initial elliptically shaped BEC for two different initial total number of atoms in the BEC, $N_T = 1.0 \times 10^6$ atoms and $N_T = 3.0 \times 10^6$ atoms respectively. Here N_f is the total number of atoms remaining in both the $0\hbar\mathbf{k}_{ph}$ and $2\hbar\mathbf{k}_{ph}$ wavepackets after the wavepackets separate. Thus, $N_f/N_T = 1 - L$ where L is the fractional loss of atoms from the mean-field due to elastic scattering. The Thomas-Fermi aspect ratio is related to the trap frequencies by $R_{aspect} \equiv x_{TF}/z_{TF} = \omega_z/\omega_x$. The actual trap frequencies in our calculation were $\nu_z = 30.7$ Hz, and $\nu_x = \nu_y = \nu_z/R_{aspect}$. The figure shows that the loss

increases as the aspect ratio decreases, and as the total number of atoms increases, reaching 60% for 3 million atoms and $R_{aspect} \approx 1/20$. N_f/N_T rises slowly to unity as R_{aspect} gets large.

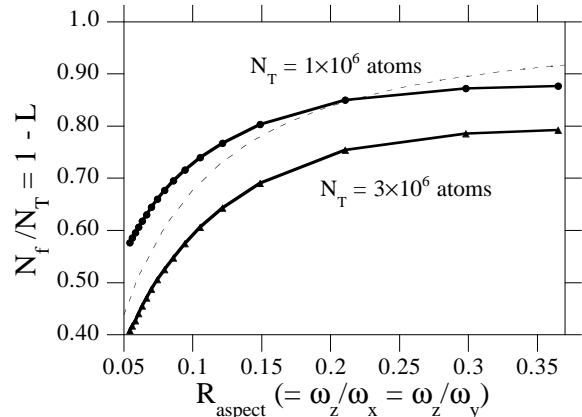


FIG. 2. Fraction of atoms remaining in the condensate wavepackets after the wavepackets have separated. A fast daughter wavepacket with half the initial number of atoms and with momentum $2\hbar k$ in the z -direction moves through the remaining parent condensate with zero central momentum. The dashed line shows the result of the heuristic model for 10^6 atoms.

A simple heuristic model helps to explain the magnitude of the losses. Assume a uniform atom density of $n = N_T/V$ in a cylinder of length $\ell = 2z_{TF}$, area $A = \pi x_{TF}^2$, and volume $V = \ell A$. If an equal number of atoms $N_T/2$ is assumed to be in the daughter and parent wavepackets, and depletion of n during the interaction is ignored, a simple argument shows that the fraction of atoms remaining after the packets separate is $(\ell_{mfp}/\ell)(1 - e^{-\ell/\ell_{mfp}})$, where $\ell_{mfp} = (\frac{n}{2}\sigma)^{-1}$ is the mean-free-path for the collision. For example, with $\nu_z = 30.7$ Hz, $R_{aspect} = 0.1$, and $N_T = 10^6$ atoms, we find that $\ell = 120 \mu\text{m}$ and $\ell_{mfp} = 140 \mu\text{m}$ are comparable in magnitude. The dashed line in Fig. 2 shows that this simple model qualitatively accounts for our results.

In the NIST 4WM experiment [8], the Na($F = 1$, $M = -1$) condensate is exposed to Raman scattering pulses which create copies of the parent condensate at central momenta $\hbar\mathbf{k}_2 = (h/\lambda_{ph})(\hat{x} + \hat{y})$ and $\hbar\mathbf{k}_3 = (2h/\lambda_{ph})\hat{x}$, leaving part of the atoms in the $\hbar\mathbf{k}_1 = \mathbf{0}$ wavepacket. The treatment of elastic scattering from the disparate momentum components of the wavepacket in the 4WM experiment is similar to the description above for the two momentum component case. Now, there are three elastic scattering loss terms for each SVE momentum component Φ_j arising due to the cross-phase modulation terms of each momentum component with the other three momentum components. We also included the momentum dependent correction term in Eq. (2) in the coupling constant for the 4WM source terms on the right hand side of Eq. (5); it only slightly decreases 4WM at large N_T . In the experiment a trap with $\nu_x = 84$ Hz, $\nu_y = 59$ Hz and

$\nu_z = 42$ Hz contained a Na BEC without a discernible non-condensed fraction. The condensate was exposed to Raman scattering pulses $600 \mu\text{s}$ after the magnetic harmonic potential was turned off. Fig. 3 shows the fraction of atoms in the 4WM output wavepacket as a function of the initial total number of atoms N_T as determined (1) experimentally (circles), (2) by calculation without including elastic scattering loss for a ratio of atoms in the three initial wavepackets of 7:3:7, and (3) by calculation including elastic scattering. The effects of elastic scattering are pronounced for large values of N_T , with the percent loss due to elastic scattering reaching 44% for 5 million atoms. The discrepancy with experiment is reduced significantly by including loss due to elastic scattering. Possible remaining sources of discrepancy include micromotion of the BEC in the time-orbiting-trap, laser misalignment and a small finite temperature component of the BEC.

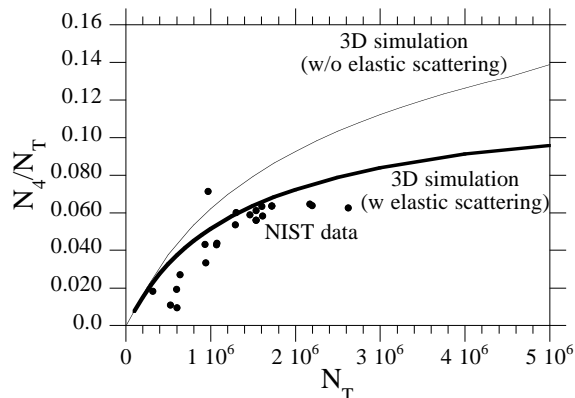


FIG. 3. Fraction of atoms in the 4WM output wavepacket, N_4/N_T , versus the number of initial atoms, N_T . The dots represent experimental data [8], the solid curve is the 3D calculation without elastic scattering, and the heavy solid curve is the 3D calculation with elastic scattering.

It is useful to put the elastic scattering discussed here into perspective. The mean-field wavefunction for the zero temperature BEC is a symmetric product of identical orbitals, each orbital being a coherent superposition of momentum wavepackets. Elastic scattering between the various momentum components of a BEC results in atoms which can not be described by the mean-field since the “modes” into which the atoms are scattered (there are an infinite number of scattering angles, or modes, to scatter into) are not macroscopically populated [16,17]. The momentum components in the spherical shell can not be generated using the dynamics of the GPE or the SVEA equations since neither contains terms that produce such momentum components. However, the SVEA equations do allow collision losses to be treated. In contrast to the formation of the spherical shell of elastically scattered atoms, the fourth wave in 4WM is explicitly generated by the GPE or the SVEA equations.

The scattering of atoms into the spherical shell and the loss of atoms from the condensate are a result of

Hamiltonian dynamics; no interactions with a bath, and therefore no incoherent processes described by T_1 or T_2 relaxation times, are necessary. Our treatment of the process has, for convenience, used an imaginary potential that serves as a mechanism to take atoms that are elastically scattered out of the condensate. It must also be noted we were able to carry out our procedure for modeling the loss of atoms from the condensate only as a result of making the slowly varying envelope approximation, by which we could track the density of atoms in each momentum wavepacket individually. As the elastic scattering loss increases, further scattering of the elastically scattered atoms with the condensate atoms will become increasingly important. This mechanism is not included in our treatment and would require following the dynamics of the elastically scattered atoms in detail.

Useful discussions with Carl J. Williams, Eite Tiesinga and Mark Edwards are gratefully acknowledged. This work was supported in part by grants from the Office of Naval Research, the US-Israel Binational Science Foundation, the James Franck Binational German-Israeli Program in Laser-Matter Interaction, the National Science Foundation through a grant for the Institute for Theoretical Atomic and Molecular Physics at Harvard University and Smithsonian Astrophysical Observatory, and the National Research Council.

-
- [1] Yu. B. Ovchinnikov *et al.*, Phys. Rev. Lett. **83**, 284 (1999).
 - [2] M. Kozuma *et al.*, Phys. Rev. Lett. **82**, 871 (1999).
 - [3] J. Stenger *et al.*, Phys. Rev. Lett. **82**, 4569 (1999).
 - [4] E. W. Hagley *et al.*, Science **283**, 1706 (1999).
 - [5] E.W. Hagley *et al.*, Phys. Rev. Lett. **83**, 3112 (1999).
 - [6] M. Trippenbach *et al.*, J. Phys. B **33**, 47 (2000).
 - [7] M. Trippenbach, Y. B. Band, and P. S. Julienne, Optics Express **3**, 530 (1998).
 - [8] L. Deng *et al.*, Nature **398**, 218-220 (1999).
 - [9] A. P. Chikkatur *et al.*, cond-mat/0003387/.
 - [10] The momentum components in the spherical shell cannot be formed by substituting Eq. (3) into $|\Psi|^2\Psi$, or by any other terms in Eq. (1).
 - [11] F. Dalfovo *et al.*, Rev. Mod. Phys. **71**, (463) (1999).
 - [12] K. Huang and C. N. Yang, Phys. Rev. **105**, 767 (1957). The real standing wave scattering wavefunction in this reference can be replaced by an incident plane wave plus outgoing scattered wave to obtain the result we have used.
 - [13] H.T.C. Stoof, M. Bijlsma and M. Houbiers, J. Res. Natl. Inst. Stand. Tech. **101**, 443 (1996); N. P. Proukakis, K. Burnett and H. T. C. Stoof, Phys. Rev. **A57**, 1230 (1998).
 - [14] M. Trippenbach, Y. B. Band, and P. S. Julienne, cond-mat/0002119.
 - [15] Y. B. Band, E. Tiesinga, J. Burke, and P. S. Julienne,

unpublished.

[16] G.D. Moore and N. Turok, Phys. Rev. **D55**, 6538 (1997).

[17] R. J. Marshall, *et al.*, Phys. Rev. **A59**, 2085 (1999).